

# Dark Matter Signals from Draco and Willman 1: Prospects for MAGIC II and CTA

---

## Torsten Bringmann

*Department of Physics, Stockholm University, AlbaNova, University Centre, S-106 91  
Stockholm, Sweden  
E-mail: troms@physto.se*

## Michele Doro

*Department of Physics G. Galilei, University of Padova & INFN, via Marzolo 8, 35131 Padova,  
Italy  
E-mail: michele.doro@pd.infn.it*

## Mattia Fornasa

*Department of Physics G. Galilei, University of Padova & INFN, via Marzolo 8, 35131 Padova,  
Italy  
Institut d'Astrophysique de Paris, boulevard Arago 98bis, 75014, Paris, France  
E-mail: mfornasa@pd.infn.it*

**ABSTRACT:** The next generation of ground-based Imaging Air Cherenkov Telescopes will play an important role in indirect dark matter searches. In this article, we consider two particularly promising candidate sources for dark matter annihilation signals, the nearby dwarf galaxies Draco and Willman 1, and study the prospects of detecting such a signal for the soon-operating MAGIC II telescope system as well as for the planned installation of CTA, taking special care of describing the experimental features that affect the detectional prospects. For the first time in such studies, we fully take into account the effect of internal bremsstrahlung, which has recently been shown to considerably enhance, in some cases, the gamma-ray flux in the high energies domain where Atmospheric Cherenkov Telescopes operate, thus leading to significantly harder annihilation spectra than traditionally considered. While the detection of the spectral features introduced by internal bremsstrahlung would constitute a smoking gun signature for dark matter annihilation, we find that for most models the overall flux still remains at a level that will be challenging to detect, unless one adopts somewhat favorable descriptions of the smooth dark matter distribution in the dwarfs.

**KEYWORDS:** Dark matter, dwarf galaxies, high energy photons.

---

## Contents

<b>1. Introduction</b>	<b>1</b>
<b>2. Phenomenology of Draco and Willman 1</b>	<b>3</b>
2.1 Draco	3
2.2 Willman 1	4
<b>3. Observations with IACTs: MAGIC II and CTA</b>	<b>4</b>
<b>4. Flux estimation</b>	<b>8</b>
4.1 Astrophysical Factor	8
4.2 Particle Physics factor and Benchmarks	11
<b>5. Results and Discussion</b>	<b>14</b>
<b>6. Conclusions</b>	<b>17</b>

---

## 1. Introduction

Even though basically nothing is known about its underlying nature, compelling evidence has accumulated in recent years that the building block of the observed structures in the universe is a new form of non-baryonic, cold dark matter (DM), with the fraction of DM to critical density being  $\Omega_{\text{DM}} \sim 0.233 \pm 0.013$  according to the most recent estimates [1]. A class of particularly well-motivated DM candidates arises in many extensions of the standard model of particle physics in the form of weakly interacting massive particles (WIMPs) that, thermally produced in the early universe, automatically acquire a relic density matching the observed DM abundance today (for reviews, see [2, 3, 4, 5]). In the following, we will restrict our analysis to the supersymmetric neutralino, which is maybe the best-motivated and the most widely studied DM candidate.

The search for DM is a vast field where different experimental techniques can provide complementary information. At the Large Hadron Collider (LHC), the detection of new supersymmetric particles through missing energy signatures, would provide valuable information about the composition of the neutralino and its role as a DM candidate (see, e.g. [6, 7]). The neutralino could also be observed through nuclear recoils in direct detection experiments. A new generation of cryogenic detectors is aiming to improve the already impressive recent limits reported by Angle et al. [8] and Ahmed et al. [9], thereby probing significant regions of the underlying parameter space. Finally, DM can be searched for through *indirect detection*, i.e. by looking for primary and secondary products (mainly gamma rays, neutrinos, positrons and anti-protons) of DM annihilation. Our attention will be focused on the detection of high-energy gamma rays.

In this field, Imaging Air Cherenkov Telescopes (IACTs) play a leading role, exploring the possibility of tracing Cherenkov photons from electromagnetic showers produced by gamma rays impinging on the Earth’s atmosphere. Ground-based gamma ray astronomy is a very active field that has matured rapidly in recent years. In the near future, new installations with improved sensitivity will investigate those regions in the sky where DM signatures can be expected. In particular MAGIC II, already in the commissioning phase, will perform observations in the northern hemisphere, while a new generation of IACTs is currently in the design phase, the Cherenkov Telescope Array (CTA), where an array of several tens of telescopes will have improved angular and energy resolution, as well as a very low energy threshold and a greatly increased sensitivity.

Dwarf spheroidal galaxies (dSphs) are the faintest known astrophysical objects believed to be dominated by DM [10]. So far, almost all detected dSphs are located in the Local Group, a fact that is most likely related to the low luminosity of these objects, ranging from  $330 L_{\odot}$  to  $3 \times 10^7 L_{\odot}$  [11, 12, 13, 14]. Typically, dSphs are satellite galaxies hosted by the halo of a larger and more massive galaxy that, in some cases, strongly influences their evolution: tidal stripping, e.g., can deprive a dSph from stars in the outer region (see, e.g., [15, 16]). While dSphs share many characteristics with stellar globular clusters — a similar number of stars (from tens to a few thousand) and a similar range in luminosity — they usually have a larger size, a fact that implies the presence of a DM halo of the order of  $10^6 - 10^8 M_{\odot}$ . The resulting mass-to-light ratios are typically larger than  $10 M_{\odot}/L_{\odot}$  and can even reach values up to  $10^3 M_{\odot}/L_{\odot}$ , suggesting that these objects are particularly interesting targets for indirect DM searches (for previous studies, see e.g., [17, 18, 19, 20, 21]).

Let us mention in passing that the number of detected dSphs is around one order of magnitude below what is expected from  $N$ -body simulations of structure formation in  $\Lambda$ CDM cosmologies, which has become known as the *missing satellites problem* [22, 23]. While many interpretations have been suggested, including the effect of decaying DM (see, e.g., [24, 25, 26] and references therein), the most natural explanation would be that the missing dSphs have so far simply escaped detection. In fact, it has been proposed that dSphs below a certain mass cannot efficiently accrete baryons, which would explain the intrinsic faintness of these objects [18]. The claimed discrepancy has recently also been mitigated considerably by the discovery of a bunch of new ultra-faint galaxies in the SDSS data [13].

In this paper, we provide an update on the possible future of the indirect detection of DM with IACTs. In particular, we discuss the prospects for the detection of DM in dSphs with MAGIC II and make tentative predictions in view of the expected characteristics of CTA. We choose to focus on two dSphs, Draco and the recently discovered ultra-faint Willman 1. While the choice of Draco is supported by the large set of available data, Willman 1 will be discussed as a very promising target for future detection.

A key ingredient in estimating the gamma ray flux for IACTs is the computation of the energy spectrum for photons produced by neutralino annihilations. In Ref. [27], it was recently shown that internal bremsstrahlung (IB) provides an important, hitherto neglected, contribution to the spectrum. While the effect of IB is largely model dependent, it appears in general as a pronounced “bump” at energies close to the kinematic cutoff at the neutralino mass. The importance of this effect is two-fold: first, the flux at high energies, where IACTs are most sensitive, is significantly increased; secondly, the introduction of spectral features allows an easier discrimination of a DM

source from potential astrophysical sources located in the vicinity, whose spectrum is usually a featureless power law. This is the first time that IB is fully included in studying prospects of DM detection for IACTs.

The paper is organised as follows: in Section 2, we will briefly review some of the main properties of Draco and Willman 1 and discuss how their DM profiles are constrained by observations. The following Section 3 is dedicated to a short description of the IACT technique, with particular attention to the features that are relevant for DM observations. In Section 4, we introduce a set of five benchmark neutralinos, representatives for the relevant regions of the parameter space, and estimate the corresponding flux based on the technical specifications for MAGIC II and CTA. Results are discussed in Section 5, and in Section 6 we present our conclusions.

## 2. Phenomenology of Draco and Willman 1

### 2.1 Draco

Draco is located at a distance of  $80 \pm 7$  kpc from the Earth [11] and is one of the best known and most often studied dSph. Discovered by Wilson [28], the first estimation of its DM content was performed only 30 years later by Aaronson [29] from the analysis of the stellar velocity dispersion. Nowadays, a large set of data is available for Draco [30, 31, 32, 33, 34]. Even though the formation of the DM halo cannot be traced back with great precision, it can be inferred that the system is composed of very old, low-metallicity stars, without any significant sign of star formation in the last 2 Gyrs. At its short distance from the Milky Way (MW) center, Draco has likely been stripped off its outermost stars in the past; today, however, no signs of tidal interactions are observed [33]. From a kinematical analysis of a sample of 200 stellar line-of-sight velocities (with radii that range from 50 pc to 1 kpc) one can infer the DM profile: The result of the fit (assuming a Navarro–Frenk–White profile, hereafter NFW [35]) indicates a virial mass of the order of  $10^9 M_\odot$  [34], with a corresponding mass-to-light ratio of  $M/L \gtrsim 200 M_\odot/L_\odot$  that characterises Draco as highly DM dominated.

Many groups have analysed the available data for Draco and modelised its DM profile [19, 20, 36, 37, 38, 39]. We are going to discuss here the two extreme cases of a *cusp* profile and a *core* profile, which span the range of possible configurations.<sup>1</sup> For the former, we take the NFW profile,

$$\rho_{\text{NFW}}(r) = \frac{\rho_s}{(r/r_s)(1+r/r_s)^2}, \quad (2.1)$$

and for the latter we take a Burkert [41, 42] profile,

$$\rho_{\text{Burkert}}(r) = \frac{\rho_s}{(1+r/r_s)(1+(r/r_s)^2)}. \quad (2.2)$$

For the scale radius  $r_s$  and the scale density  $\rho_s$ , we use the values summarised in Table 1 (taken from Ref. [39]). Note that both profiles produce good fits to the velocity dispersion profiles, down to the pc scales where the innermost stars are observed. No direct observational information is available for distances even closer to the centre, where the two profiles differ significantly.

---

<sup>1</sup>It should be underlined that core profiles are not compatible with current CDM simulations: recent results predict DM halos well-fitted by an Einasto profile without converging to a precise value for the inner slope [40]. For comparison with previous studies, however, we chose to still include core profiles in the analysis.

	Draco–Burkert	Draco–NFW	Willman 1–NFW
$r_s$ (kpc)	0.35	0.50	0.18
$\rho_s$ ( $M_\odot/\text{kpc}^3$ )	$3.6 \times 10^8$	$1.3 \times 10^8$	$4.0 \times 10^8$
$\theta_{90}$ ( $^\circ$ )	$0.52^\circ$	$0.35^\circ$	$0.20^\circ$
$D$ (kpc)	$80 \pm 7$		$38 \pm 7$

**Table 1:** Scale radius (kpc) and scale density ( $M_\odot/\text{kpc}^3$ ) that appear in the DM density profiles. The NFW and the Burkert profiles in the case of Draco represent models N3 and B2, respectively, from Ref. [39]. In the case of Willman 1, the NFW fit is taken from Ref. [52]. In addition, the semi-aperture of the solid angle corresponding to 90% of emission  $\theta_{90}$  ( $^\circ$ ) is reported together with the target distance  $D$  (kpc).

Possible DM annihilation signals from Draco have already been searched for in the past: after the CACTUS experiment had claimed the detection of an excess of  $\sim 7000$  high-energy photons in only 7 hours [43], almost all IACTs tried to reproduce the result, but the claim was not confirmed [44, 45]. MAGIC observed Draco for 7.8 hours during 2007 above 140 GeV [46]. Within a  $2\sigma$  confidence limit, the collaboration reported an upper limit for the integral flux of  $\Phi^{u.l.}(E > 140 \text{ GeV}) < 1.1 \times 10^{-11} \text{ ph cm}^{-2} \text{ s}^{-1}$ .

## 2.2 Willman 1

Willman 1 (SDSS J1049+5103) is a very peculiar object, located at a distance of  $38 \pm 7$  kpc from the Earth in the constellation of Ursa Major. Discovered in 2004 by B. Willman [47, 48], using data from the Sloan Digital Sky Survey [49], it was then further observed with Keck/DEIMOS [50] and more recently by Siegel et al. [51]. With an absolute magnitude of  $M_V \sim -2.5$  and a half-light radius (i.e. the radius of a cylinder, pointing to the Earth, that encloses half of the luminosity of the object) of  $21 \pm 7$  pc, it looks very similar to a globular cluster, even if its narrow distribution of stellar velocities and the large spread in stellar metallicities suggests that it is indeed the smallest dSph ever observed. The object may show evidence for tidal disruption from its tri-axial stellar distribution [48]. On the other hand, the difference in the stellar luminosity function between the central and outermost stars reveals a strong mass segregation. With a luminosity of  $855 L_\odot$ , and a mass of the order of  $5 \times 10^5 M_\odot$  [50], Willman 1 could feature a mass-to-light ratio in the range  $500 - 700 M_\odot/L_\odot$ , or even more, making it one of the most DM dominated objects in the Universe [52].

The small number of stars that belong to this dSph hinders, however, an accurate determination of the DM density profile. Following Strigari et al. [52], we parametrise its DM halo with an NFW profile, as specified in Table 1, although these parameters are subject to somewhat larger uncertainties than in the case of Draco.

## 3. Observations with IACTs: MAGIC II and CTA

When entering into the atmosphere, cosmic gamma rays (as well as the many orders of magnitude more frequent background charged cosmic rays) quickly lose energy through interactions with the nuclei of atmospheric molecules, dominantly by pair production of electrons and positrons. Bremsstrahlung photons radiated by these highly energetic electrons and positrons in turn lead to

the production of secondary electron-positron pairs, thus triggering the subsequent development of a particle shower. When the electron-positron energy falls below  $E_c \approx 83$  MeV in the atmosphere, the dominant mechanism of energy loss becomes ionization and the shower rapidly dies off. This takes place at an altitude of 8 – 12 km, depending on the energy of the primary gamma ray. This cascade of highly relativistic particles causes a flash of UV-blue Cherenkov light, with the greatest emission coming from the shower maximum (i.e. where the number of free electrons and positrons is maximal), lasting a few nanoseconds and propagating in a cone with an opening angle of  $\sim 1^\circ$ , slightly depending on the primary energy. The resulting circle of projected light at 2000 m asl (the MAGIC telescope altitude) has a radius of about  $\sim 120$  m. If a telescope is located inside this Cherenkov-light pool, the light can be reflected from the collecting mirrors and focused onto a multi-pixel recording camera. An image reconstruction algorithm [53] then allows the recovery of the energy and direction of the primary particle, and determines whether it was more likely a hadron or a photon. In this way, it is possible to reject up to 99% of the background, constituted mainly by sub-showers generated by charged cosmic ray particles, by muons and by the night sky background light.

This technique was pioneered by the Whipple telescope [54], with several successors currently operating, including MAGIC, HESS, CANGAROO-III and VERITAS<sup>2</sup>. In this paper, we will address observational prospects for the upcoming MAGIC II telescope system and for the future generation of IACTs, focusing on the case of CTA. MAGIC II is a stereoscopic system of telescopes, composed of MAGIC and a second telescope currently under commissioning on the island of La Palma, which will start operation in 2009. The stereoscopic view of two telescopes (pioneered by HEGRA [55]), together with the improved technical characteristics of the second detector, will allow a general improvement in the overall performance of the experiment, in particular in terms of energy and angular resolution, as well as energy threshold. The performance of the MAGIC II array was simulated with Monte Carlo (MC) tools by Carmona et al. [56]. CTA, on the other hand, is the result of an effort for a next generation Cherenkov observatory with increased capabilities: normally, one single telescope can cover 1.5–2 orders of magnitude in energy range. With the combined use of many telescopes of 2–3 different sizes, CTA should be able to extend the energy range to almost 4 orders of magnitude, from roughly  $\sim 30$  GeV to  $\sim 100$  TeV. The experiment is still in the early design phase and the final layout of the array is thus far from defined yet; the performance, therefore, is still subject to changes. For this paper, we will refer mainly to the work of Bernlöher et al. [57] and several private communications within the collaboration. The CTA prototype construction could start in 2010, at least for some of the main components, and the final installation is foreseen in 2012–15.

The performance of an IACT in terms of its prospects to detect a DM annihilation signal can generally be characterised by a small number of basic parameters, which are described in the following (see also Table 2 for a summary of the characteristics for MAGIC II and CTA):

- *Energy threshold:* The energy threshold of an IACT can take slightly different values according to the definition. Hereafter we consider it to be the peak of the reconstructed MC energy distribution (other definitions being analysis threshold, trigger threshold, etc.). This value de-

---

<sup>2</sup>See, respectively, <http://www.magic.mppmu.mpg.de>, <http://www.mpi-hd.mpg.de/htm/HESS>, <http://icrh9.icrr.u-tokyo.ac.jp/> and <http://veritas.sao.arizona.edu/>

depends mainly on the reflector area of the telescope: A larger mirror area allows, in particular, to collect more photons from the showers and thus increases the chance of discrimination against the night sky background light, in particular for low energy showers. The use of a stereoscopic system also plays an important role because it enhances the gamma/hadron ( $g/h$ ) discrimination power which is weaker at low energy. The energy threshold changes with the zenith angle of observation, and sources culminating high in the sky are preferred. Reaching a low energy threshold is an important feature for DM studies with IACTs, both because of the increased number of photons and because of the enhanced possibility to observe the spectral cutoff even for low-mass neutralinos. Making use of stereoscopic observations, MAGIC II will have an energy threshold of 60-70 GeV [56], with possible extension to even lower energies with improved analysis techniques and new trigger systems currently under development [58]. This value will be further lowered to at least 30 GeV for CTA. The telescope acceptance for gamma rays around 30 GeV starts to decrease rapidly, but a very strong gamma ray signal could probably even be detected at energies as low as about 10 GeV.

- *Energy resolution:* The true energy of the primary gamma ray  $E'$  is reconstructed on the basis of a comparing analysis between the shower image parameters and MC events. The probability to assign, after the analysis, an energy  $E$  to the primary gamma ray can be approximated by

$$R_\epsilon(E - E') \approx \frac{1}{\sqrt{2\pi}E} \cdot \exp\left(-\frac{(E - E')^2}{2\epsilon^2 E^2}\right). \quad (3.1)$$

Typical values for the energy resolution  $\epsilon$  are of the order of 10-30% for IACTs, depending on the energy. The reason for such large uncertainties is the combined effect of many sources of uncertainties (for a more detailed discussion, see Ref. [46]). The energy resolution is an important parameter when observing spectral features as bumps and cutoffs that can provide clear signatures for a DM signal. MAGIC II will have an energy resolution of 15% above 300 GeV (up to 20% at 70 GeV); for the CTA, this situation could radically improve. Finally, let us note that further systematic errors might hide in the absolute energy calibration; the recent MAGIC observation of a clear cutoff in the Crab Nebula spectrum<sup>3</sup>, when compared to a corresponding future observation by Fermi-LAT [59], may allow for the first robust calibration of gamma ray energies [60].

- *Angular resolution:* The reconstruction of the direction of a primary gamma ray is performed through image analysis. As a result, a gamma ray coming from a direction  $\psi'$  will be reconstructed to a direction  $\psi$  in the sky with a probability distribution that can be fitted to a Gaussian function:

$$B_{\vartheta_r}(\psi' - \psi) = \frac{1}{2\pi\vartheta_r^2} \cdot \exp\left(-\frac{(\psi' - \psi)^2}{2\vartheta_r^2}\right). \quad (3.2)$$

---

<sup>3</sup>The Crab Nebula is a supernova remnant that is conventionally taken as reference source for cross-calibrations in gamma ray astronomy due to its very stable and intense flux.

The standard deviation  $\vartheta_r$  of the Gaussian corresponds to the telescope angular resolution, also called Point Spread Function (PSF). As a consequence, any source will appear somewhat blurred. The stereoscopic system exploited in MAGIC II will improve the PSF, allowing values as low as  $0.05^\circ$ , while for CTA we expect an even smaller PSF. It is hard to predict an exact value given the current lack of knowledge of the CTA design, but a realistic value that we use for this study is  $0.02^\circ$  (see also [61]). For extended sources, as in the case of dSphs, the PSF plays an important role in the reconstruction of the DM density profile, as discussed in the next section.

- *Flux sensitivity*: The sensitivity of an IACT is usually defined as the minimum flux for a  $5\sigma$  detection over the background, after 50 hours of observation time and based on at least 10 collected photons. For operating experiments, the sensitivity can be computed by using real data and following Eq. 17 of [62], while for planned experiments the sensitivity has to be estimated on the basis of MC simulations and is therefore subject to larger uncertainties. The procedure is as follows: a full data analysis is performed on two samples of MC simulations, one for gamma ray events and one for background events (basically protons and helium), during which a number of parameters (“cuts”) is optimised to maximise the analysis quality factor  $Q = \epsilon_\gamma / \sqrt{\epsilon_h}$ , i.e. the ratio between the efficiency for gamma rays and the square root of the hadron efficiency (“efficiency” referring here to the ratio between the number of events passing the analysis cuts and the number of events at MC, input, level). After the optimisation, one can estimate the number of hadrons  $N_h(> E)$  above some energy  $E$ . Given the Poissonian distribution of events, a  $5\sigma$  detection is obtained whenever the number of gamma rays detected is larger than  $5\sqrt{N_h(> E)}$ . The integrated sensitivity above  $E$  is thus given by:

$$\Phi^{min}(> E) = \frac{5\sqrt{N_h(> E)}}{A \cdot t_{50}} \frac{1}{\epsilon_\gamma}, \quad (3.3)$$

where  $A$  is the MC gamma ray simulation area and  $t_{50}$  is the time interval corresponding to 50 hours.

$N_h(> E)$  and  $\epsilon_\gamma$ , and thus the sensitivity, are usually determined assuming a featureless power law spectrum of MC gamma ray events of index  $-2.6$ . This corresponds approximately to the spectrum of the Crab. For this reason, the sensitivity is often also expressed in terms of “Crab” units (C.U). In the case of the benchmark neutralinos under study (see next section), the gamma ray spectra are usually harder than that of the Crab and no longer featureless; it is therefore natural to ask how much this would change the sensitivity.

To address this question, let us note that the sensitivity mainly depends on the  $g/h$  discrimination power. The  $g/h$  separation, however, is very efficient at intermediate and large energies, where the shower parameters are firmly distinguishable between hadronic and gamma events. At energies below  $\sim 30$  GeV, on the other hand, the differences are more subtle and the sensitivity *is* affected. Hence we expect that the differential sensitivity does not depend too strongly on the spectrum of the source, unless in the case of rather low energies. An exact treatment of this effect would require dedicated studies with MC simulations, which is

	MAGIC	MAGIC II	CTA*
$E_0$ (GeV)	100	70	30
$\epsilon$	30-20%	20-10%	10%
$\vartheta_r$ ( $^\circ$ )	0.10 $^\circ$	0.05 $^\circ$	0.02 $^\circ$
$S(> E_0)$ ( $\text{cm}^{-2} \text{s}^{-1}$ )	$5 \times 10^{-11}$	$1.4 \times 10^{-11}$	$1.5 \times 10^{-11}$

**Table 2:** Comparison of the performance of the MAGIC, MAGIC II and CTA\* telescopes.  $E_0$  (GeV) is the energy threshold,  $\epsilon$  the energy resolution and  $\vartheta_r$ ( $^\circ$ ) the angular resolution. The sensitivity  $S(> E_0)$  ( $\text{cm}^{-2} \text{s}^{-1}$ ) is given for a Crab-like spectrum above the energy threshold.

\*For CTA, the numbers have to be taken as placeholders because the telescope design is not yet fixed.

beyond the aim of this work. Based on a preliminary MC analysis, however, we generally expect that the sensitivity at a given energy will not change by more than a factor of two compared to that defined for the Crab. A full analysis of this effect is left for future work.

## 4. Flux estimation

The gamma ray flux from DM annihilation can be factorised into two different contributions:

$$\frac{d\Phi}{dE} = J(\psi) \cdot \frac{d\Phi^{PP}}{dE}. \quad (4.1)$$

The term  $J(\psi)$ , also called the *astrophysical factor*, depends on the DM morphology at the emission region. The *particle physics factor*  $d\Phi^{PP}/dE$ , on the other hand, depends on the microscopic properties of the DM candidate, in particular its mass and cross section, as well as the annihilation modes and branching ratios, that define the gamma ray spectrum. For a given telescope energy threshold  $E_0$ , the integral flux is thus  $\Phi(> E_0) = J \cdot \Phi^{PP}(> E_0)$ .

The ability to reconstruct the two factors depends on the experimental performance of the IACT; in the following, we will estimate the expected flux for Draco and Willman 1.

### 4.1 Astrophysical Factor

The astrophysical factor depends on the source distance and geometry (as well as the PSF of the telescope), but for a given DM profile it does not depend on the particular DM candidate. As a consequence, the discussion here remains valid for any generic WIMP candidate. Pointing the telescope towards a direction  $\psi$  in the sky, and taking into account its finite angular resolution, the astrophysical factor is given by:

$$J(\psi) = \frac{1}{4\pi} \int d\Omega \int d\lambda \left[ \rho^2(r(\lambda, \psi)) \cdot B_{\vartheta_r}(\theta) \right], \quad (4.2)$$

where the angular integration  $d\Omega = d\varphi d(\cos \theta)$  extends over a cone centered around  $\psi$ , with an opening angle a few times the PSF  $\vartheta_r$ . The integration over  $\lambda$  is along the line-of-sight, in the direction  $\psi$ , such that  $r = \sqrt{\lambda^2 + D^2 - 2D\lambda \cos(\Psi)}$ , where  $D$  is the distance of the source from the Sun and  $\cos(\Psi) \equiv \cos(\theta) \cos(\psi) - \cos(\varphi) \sin(\theta) \sin(\psi)$ . Defined as above,  $J(\psi)$  is conventionally expressed in units of  $M_\odot^2 \text{kpc}^{-5} \text{sr}^{-1}$  or  $\text{GeV}^2 \text{cm}^{-5} \text{sr}^{-1}$ . In order to translate it to the dimensionless

$\tilde{J}$	Draco–Burkert	Draco–NFW	Willman 1–NFW
(GeV <sup>2</sup> /cm <sup>5</sup> )	$3.84 \times 10^{17}$	$4.71 \times 10^{17}$	$9.55 \times 10^{17}$
(M <sub>⊙</sub> /kpc <sup>5</sup> )	$8.63 \times 10^{10}$	$1.06 \times 10^{11}$	$2.15 \times 10^{11}$

**Table 3:** Comparison of the integrated astrophysical factor  $\tilde{J}$  for Draco and Willman 1, for the profiles specified in 1.

quantity  $J(\psi)$  as defined in Ref. [63], one simply has to multiply it by  $5.32 \times 10^{-21}$  GeV<sup>-2</sup>cm<sup>5</sup>sr (=  $2.37 \times 10^{-14}$  M<sub>⊙</sub><sup>-2</sup>kpc<sup>5</sup>sr).

Integrating Eq. 4.2 over the full angular extension of the source gives:

$$\tilde{J} \equiv \int d\Omega_\psi J(\psi) \simeq \frac{1}{4\pi D^2} \int dV \rho^2(r), \quad (4.3)$$

where the second integral is over the *spatial* extent of the source. Note that this expression is now given in units M<sub>⊙</sub><sup>2</sup> kpc<sup>-5</sup> (or GeV<sup>2</sup> cm<sup>-5</sup>) and no longer depends on the telescope PSF.

Using the DM profile parameters of Table 1, we now show in Figure 1 the quantity  $J(\psi)$  for Draco and Willman 1. While the two sources, from this plot, appear similar in terms of their angular size  $\psi$ , we recall that their spatial extension is quite different: By comparing, e.g., their respective scale radii for an NFW profile, one sees that Willman 1 ( $r_s = 0.18$  kpc) is considerably smaller than Draco ( $r_s = 0.50$  kpc). In the case of Draco, the cusp and core profiles are almost identical (up to an overall normalisation factor of  $\sim 2$ ) for angular distances larger than about  $\psi \sim 0.3^\circ$ , below which the cusp profile starts to increase more rapidly. At the center, the two profiles differ by around one order of magnitude, the difference increasing with decreasing PSF. Whenever an extended emission would be observed, one could thus in principle be able to discriminate between different profiles by comparing the flux at different distances from the center. As it becomes obvious from Figure 1, and as already stressed by Sanchez–Conde et al. [20], the angular resolution of the telescope would play an important role in this case. Taking into account the full range of profiles consistent with the observational data [52], we note that the astrophysical factor for dSphs is far better constrained than for, e.g., the galactic center, where the uncertainty in the inner part spans several orders of magnitude [64].

Given a telescope PSF of the order of  $0.1^\circ$ , and the expected feebleness of the signal, however, the capability of reconstructing the morphology of extended sources is very limited. This is particularly true in the case of non-stereo IACTs where the shower direction is reconstructed with less precision. Even when making the rather optimistic assumption that a signal could be discriminated against the background out to a distance where the annihilation flux is a factor of 3 less than from the direction towards the center, the source would appear at a size of only roughly twice the PSF for both Draco and Willman 1, in the case of a cuspy profile. For a core profile, the same measure would indicate an apparent extension out to  $\lesssim 0.2^\circ$ , still well contained in a normal IACT camera ( $\sim 3^\circ$  aperture). As we will see, the expected annihilation fluxes are rather low and we find it therefore premature to discuss in depth the possibilities to distinguish between different profiles in the way indicated above; rather, we will in the following focus on the total, i.e. integrated, flux.

Table 3 reports the calculation of the *integrated* astrophysical factor  $\tilde{J}$  for the two dSphs studied here. For Willman 1, the uncertainty in the DM profile translates into a 95% confidence interval of

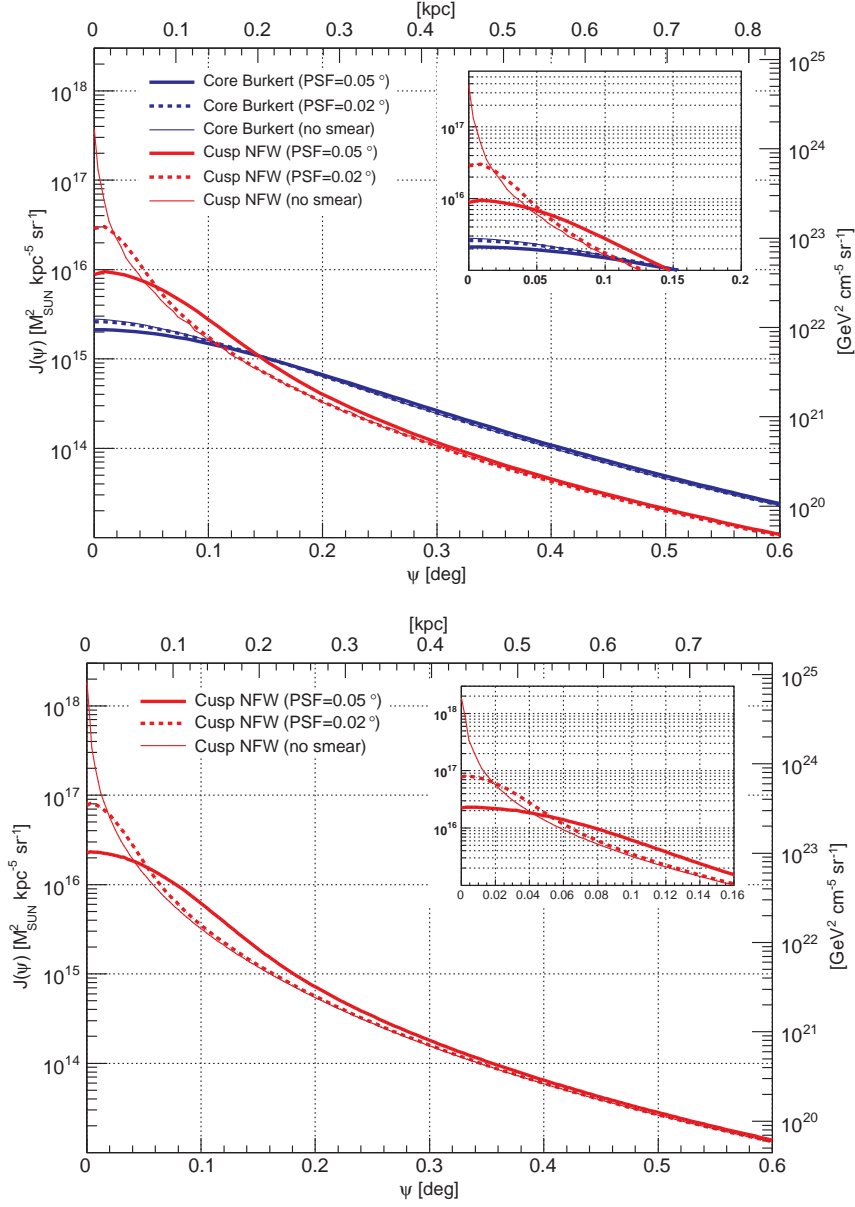


**Figure 1:** The  $J(\psi)$  factor in the case of Draco (upper plot) and Willman 1 (lower plot). Core profiles are shown in blue, cusp profiles in red. Thick solid (dashed) lines represent profiles smeared with the MAGIC II (CTA) angular resolution. Thin solid lines represent the profiles without smearing. The upper right panel in each figure shows a zoom-in of the region close to the center. For comparison, we also show the profiles for a hypothetical, infinite angular resolution.

about  $8 \times 10^{17} \text{ GeV}^2/\text{cm}^5 \lesssim \tilde{J} \lesssim 4 \times 10^{19} \text{ GeV}^2/\text{cm}^5$  [52]. In the case of Draco, the astrophysical factor lies in the range  $10^{17} \text{ GeV}^2/\text{cm}^5 \lesssim \tilde{J} \lesssim 2 \times 10^{18} \text{ GeV}^2/\text{cm}^5$  [21]. Again, these astrophysical uncertainties are rather small when compared to other potential sources of DM annihilation signals – but one should keep in mind that our choices of DM profiles are actually quite conservative: taking into account the above quoted range of possible values for  $\tilde{J}$  that are consistent with current

BM	$m_{1/2}$	$m_0$	$\tan\beta$	$A_0$	$s(\mu)$	$m_\chi$	$\Omega_\chi h^2$	$\sigma v _{v=0}$
$I'$	350	181	35.0	0	+	141	0.12	$3.6 \cdot 10^{-27}$
$J'$	750	299	35.0	0	+	316	0.11	$3.2 \cdot 10^{-28}$
$K'$	1300	1001	46.0	0	-	565	0.09	$2.6 \cdot 10^{-26}$
$F^*$	7792	22100	24.0	17.7	+	1926	0.11	$2.6 \cdot 10^{-27}$
$J^*$	576	108	3.8	28.3	+	233	0.08	$9.2 \cdot 10^{-29}$

BM	$r$	$2 \cdot \sigma v _{\gamma\gamma}$	$\sigma v _{Z\gamma}$	$\Phi_{>70 \text{ GeV}}^{PP}$	$\Phi_{>30 \text{ GeV}}^{PP}$
$I'$	4	$7.9 \cdot 10^{-30}$	$8.5 \cdot 10^{-31}$	$1.6 \cdot 10^{-33}$	$9.9 \cdot 10^{-33}$
$J'$	34	$3.4 \cdot 10^{-30}$	$4.1 \cdot 10^{-31}$	$2.2 \cdot 10^{-34}$	$1.1 \cdot 10^{-33}$
$K'$	<0.1	$1.8 \cdot 10^{-31}$	$2.2 \cdot 10^{-32}$	$1.5 \cdot 10^{-32}$	$7.5 \cdot 10^{-32}$
$F^*$	11	$5.8 \cdot 10^{-30}$	$1.6 \cdot 10^{-29}$	$9.6 \cdot 10^{-34}$	$2.4 \cdot 10^{-33}$
$J^*$	2300	$5.5 \cdot 10^{-30}$	$1.8 \cdot 10^{-30}$	$7.9 \cdot 10^{-34}$	$8.9 \cdot 10^{-34}$

**Table 4:** Parameters defining the benchmark models and some relevant quantities related to the annihilation spectrum.  $m_{1/2}$  and  $m_0$  (expressed in GeV) are the uniform masses of gauginos and scalars, respectively.  $\tan\beta$  is the ratio between the vacuum expectation values of the two Higgs bosons.  $A_0$  (in GeV) is the coefficient of the trilinear scalar term and  $\mu$  is the coefficient of the mass term in the Higgs potential.  $m_\chi$  (in GeV) is the neutralino mass,  $\Omega_\chi h^2$  its relic density and  $\sigma v|_{v=0}$  (expressed in  $\text{cm}^3 \text{s}^{-1}$ ) its annihilation rate today.  $r$  is the ratio of IB photons over secondary photons (above  $0.6 m_\chi$ ) and  $\sigma v|_{\gamma\gamma}$ ,  $\sigma v|_{Z\gamma}$  are the annihilation rates for the  $\gamma$  lines.  $\Phi^{PP}$  (expressed in  $\text{cm}^3 \text{s}^{-1} \text{GeV}^{-2}$ ), finally, is defined in Eq. 4.4 and given for MAGIC II ( $E_0 = 70$  GeV) and CTA ( $E_0 = 30$  GeV) energy thresholds, respectively.

observations of velocity dispersions in the dwarfs, one could thus win a factor of up to about 4 (in the case of Draco) or 40 (in the case of Willman 1) in the annihilation flux; we will get back to this in Section 5.

## 4.2 Particle Physics factor and Benchmarks

The particle physics factor in Eq. 4.1 is given by:

$$\frac{d\Phi^{PP}}{dE} = \frac{\sigma v}{2m_\chi^2} \cdot \sum_i B^i \int dE' \frac{dN_\gamma^i(E')}{dE'} R_\epsilon(E - E'), \quad (4.4)$$

where  $\sigma v$  is the total annihilation rate of the DM particles,  $m_\chi$  the mass of the DM particle,  $B_i$  the branching ratio into channel  $i$  and  $dN_\gamma^i/dE$  the corresponding differential number of photons per (total) annihilation. The integration over  $R_\epsilon(E - E')$  (see Eq. 3.1), takes into account the finite energy resolution of the instrument. The *total* number of photons above some energy  $E_0$  of course no longer depends on the energy resolution (as long as  $1 - E_0/M_\chi \gg \epsilon$ ) and is given by:

$$N_\gamma(> E_0) \simeq \sum_i B^i \int_{E_0}^{m_\chi} \frac{dN_\gamma^i(E)}{dE} dE. \quad (4.5)$$

Three different contributions to the spectrum can, in general, be distinguished: first of all *monochromatic  $\gamma$  lines*, where photons are primary products of neutralino annihilation through the reactions  $\chi\chi \rightarrow \gamma\gamma$  and  $\chi\chi \rightarrow \gamma Z^0$  [63]. These processes are very model-dependent; while providing a striking experimental signature, they are usually subdominant (for a recent analysis,

see [27]). As a further contribution, *secondary photons* are produced in the hadronization and further decay of the primary annihilation products, mainly through the decay of neutral pions, resulting in a featureless spectrum with a power law like behaviour at small photon energies and a rather soft cutoff at  $m_\chi$ . These contributions, which always dominate the total spectrum at low energies, are highly model-independent and have a spectral shape that is almost indistinguishable for the various possible annihilation channels (see, e.g., [4, 64]).

For charged annihilation products, a third contribution has to be included; *internal bremsstrahlung*, where an additional photon appears in the final state. As has been pointed out recently [27], these photons generically dominate the total spectrum at energies close to the kinematical cutoff at  $m_\chi$ . Moreover, they add pronounced signatures to the spectrum that would allow for a clear identification of the DM origin of an observed source; viz. a very sharp cutoff at  $m_\chi$  and bump-like features at slightly smaller energies. While photons directly radiated from charged final states give rise to a rather model-independent contribution [65], photons radiated from charged virtual particles strongly depend on the details of the underlying DM model.

As anticipated in the introduction, for what concerns the particle physics content, we will restrict ourselves to supersymmetric DM. While the Minimal Supersymmetric Standard Model (MSSM) needs more than 100 parameters for its full characterisation, in the following we will only consider a constrained version, minimal supergravity (mSUGRA – see, e.g., [66]), where gravity is supposed to mediate SUSY breaking and the number of parameters is reduced to 4 plus a choice of sign after certain commonly adopted, physically well-motivated assumptions such as neglecting  $CP$  violating or flavour-changing neutral current interactions and imposing the grand unification theory (GUT) condition for the gauge couplings,  $M_1 = 5/3 \tan^2 \theta_w M_2 \approx 0.5 M_2$ . The parameters defining an mSUGRA model are: universal masses for gauginos ( $m_{1/2}$ ) and scalars ( $m_0$ ), a common trilinear coupling term  $A_0$  in the SUSY breaking part of the Lagrangian, the ratio  $\tan \beta$  of the vacuum expectation values of the two Higgs bosons and the sign for the coefficient  $\mu$  of the mass term in the Higgs potential. By solving the renormalisation group equations, these parameters, defined at the GUT scale, can be translated into masses and couplings at observable, i.e. low, energies.<sup>4</sup>

Even if highly constrained, these models permit a rich phenomenology. From a cosmological point of view, one can single out five regions of the underlying parameter space that are particularly interesting as they correspond to models with a neutralino relic density in accordance with the value measured by WMAP: the *bulk region* at low  $m_0$  and  $m_{1/2}$ , where the mass spectrum contains light sleptons  $\tilde{\ell}$  and, as a consequence, the relic density is mainly determined by annihilation processes  $\chi\chi \rightarrow \ell^+\ell^-$  in the early universe (through a  $t$ -channel exchange of  $\tilde{\ell}$ ); the *funnel region* at intermediate values for  $m_0$  and  $m_{1/2}$ , where  $m_A \approx 2m_\chi$  and annihilations in the early universe are thus enhanced by the presence of the near-resonant pseudo-scalar Higgs boson; the hyperbolic

---

<sup>4</sup>For the calculation of the low-energy features of these models (i.e. mass spectra etc.), we use version 4.01 of DarkSUSY [67] that relies on the public code Isajet 7.69 [68]. One should be aware, however, that these calculations are highly sensitive to how the renormalisation group equations are implemented and different codes, or even different versions of the same code, may give rather different results (see, e.g., Battaglia et al., 2001; 2004b). Typically, the *qualitative* low-energy features of a given model can still easily be reconstructed by allowing for slight shifts in the parameter space (defined at high energies). From a practical point of view, this situation therefore does not constitute a severe problem as one may always regard a set of low-energy quantities like the mass spectrum, annihilation cross section and branching ratios as a valid *effective* definition of the model.

branch or *focus point region*, where  $m_0 \gg m_{1/2}$  and the neutralino becomes an almost pure Higgsino, with large annihilation rates into gauge bosons; the *stau coannihilation region* at large  $m_{1/2}$  but small  $m_0$ , where  $m_\chi \approx m_{\tilde{\tau}}$  and coannihilations with staus (and usually other sleptons as well) are important in determining the relic density; and finally the *stop coannihilation region* (arising when  $A_0 \neq 0$ ) where  $m_\chi \approx m_{\tilde{t}}$ .

In what follows, we choose to work with a set of benchmark models, representative of the different regions in parameter space described above. From an experimental point of view, the advantage of benchmark models is that they allow a direct comparison between data from different experiments (most of the benchmarks that we use have already been extensively studied in other contexts) and, in general, a more detailed *per case* analysis than for, e.g., parameter scans. Our particular choice of benchmark models is summarised in Table 4.

The features of these models that are important in our context are the following:

- $I'$ : This model (like the following two) was introduced by Battaglia et al. [69], where also its phenomenology at colliders was extensively studied. It is a typical example of a model in the *bulk region*. While the annihilation into lepton pairs is strongly suppressed for neutralinos with the small velocities they exhibit today (unlike in the early universe), annihilation into  $\ell^+ \ell^- \gamma$ , which does not suffer from helicity suppression [70], gives a considerable contribution due to the lightness of the sleptons.
- $J'$ : This model lies in the *coannihilation tail*. The sleptons being close to degenerate with the neutralino, IB from lepton final states gives even higher enhancement of the flux than in the previous case.
- $K'$ : A representative model for the *funnel region*, where the annihilation dominantly occurs through an  $s$ -channel pseudo-scalar Higgs boson. Consequently, the additional emission of a photon does not lift the helicity suppression in this case and therefore IB contributions have to be subdominant.
- $F^*$ : Introduced in Ref. [27] as BM4, this model exhibits a large neutralino mass, as typical in the *focus point* region. In this regime, the chargino is close to degenerate with the neutralino (in this case an almost pure Higgsino) and large IB contributions result from charged gauge boson final states [71].
- $J^*$ : Introduced in Ref. [27] as BM3, this is another example of a neutralino in the coannihilation region, characterised by a particularly large IB contribution.

We used DarkSUSY, which in its most recent public release 5.0.1 [72], contains a full implementation of the IB contributions focused on here, to compute the annihilation spectra for the benchmark models defined above. Line signals are also taken into account, but they turn out to be completely subdominant in the cases studied here (except for model  $F^*$ ). The resulting spectra are plotted in Figure 2, both before taking into account the finite energy resolution of the detector and for the case of an energy resolution of 10%. The main characteristics of these spectra are also summarised in Table 4.

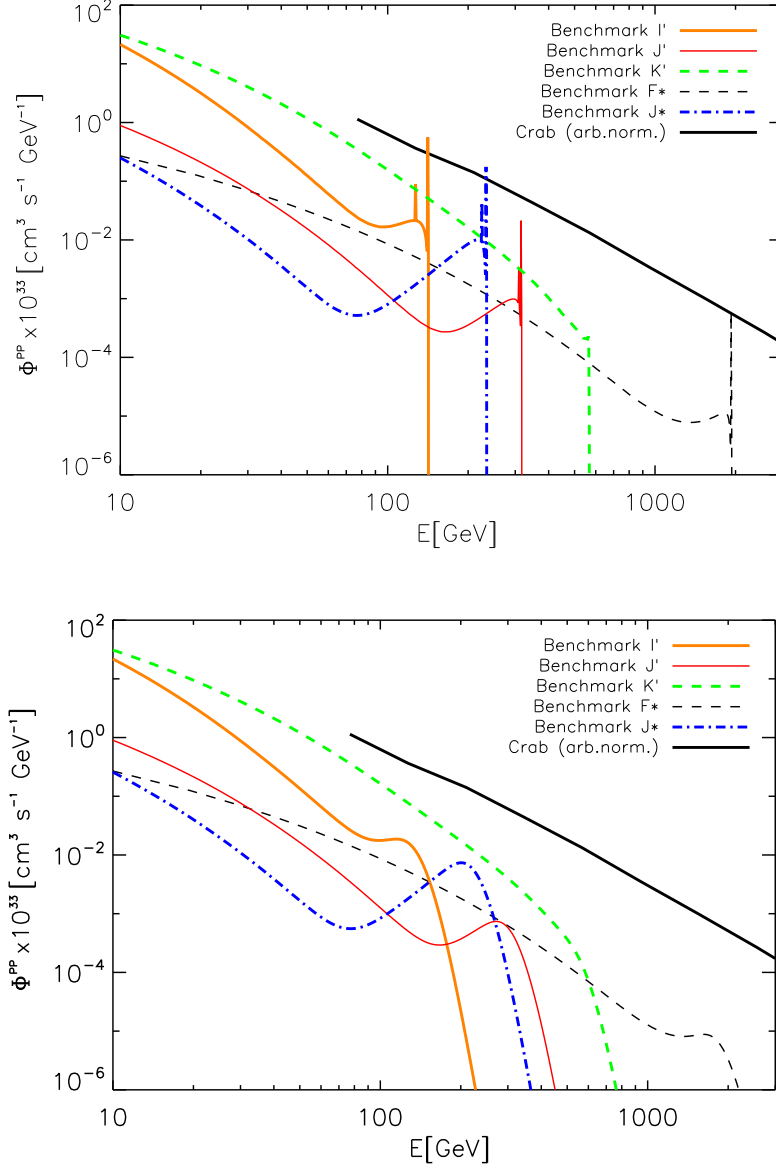


**Figure 2:** The particle physics factor  $d\Phi^{PP}/dE$ , as defined in Eq. 4.4, for the benchmarks models introduced in Section 4.2. The upper panel shows the case of a hypothetical detector with perfect energy resolution, and a line width of  $\epsilon \sim \nu \sim 10^{-3}$ , while the lower case shows the more realistic example of  $\epsilon = 10\%$ . For comparison, we also show the spectrum of the Crab Nebula, taken from Ref. [46] with an arbitrary normalisation.

## 5. Results and Discussion

Combining the astrophysical factor of Table 3 and the particle physics factor from Table 4, we can finally make predictions about the expected gamma ray flux above the telescope energy threshold  $E_0$ . A summary of the results is reported in Table 5, where we also quote the increase in the overall flux normalization that would be necessary to meet the required sensitivity for a  $5\sigma$  detection

Draco-NFW				
	MAGIC II		CTA <sub>30</sub>	
$I'$	0.75	( $1.9 \cdot 10^4$ , $1.3 \cdot 10^4$ , <b>2900</b> )	4.7	(3100, 2100, <b>490</b> )
$J'$	0.10	( $1.4 \cdot 10^5$ , $3.2 \cdot 10^4$ , <b>7600</b> )	0.52	( $2.8 \cdot 10^4$ , 4900, <b>1200</b> )
$K'$	7.0	(2000, 2000, <b>470</b> )	35	(410, 260, <b>61</b> )
$F^*$	0.45	( $3.1 \cdot 10^4$ , $1.6 \cdot 10^4$ , <b>3800</b> )	1.1	( $1.3 \cdot 10^4$ , 2800, <b>670</b> )
$J^*$	0.37	( $3.8 \cdot 10^4$ , 7400, <b>1700</b> )	0.42	( $3.4 \cdot 10^4$ , 1200, <b>290</b> )
Willman 1				
	MAGIC II		CTA <sub>30</sub>	
$I'$	1.5	(9200, 6200, <b>150</b> )	9.4	(1500, 1000, <b>25</b> )
$J'$	0.21	( $6.9 \cdot 10^4$ , $1.6 \cdot 10^4$ , <b>380</b> )	1.1	( $1.4 \cdot 10^4$ , 2400, <b>58</b> )
$K'$	14	(990, 990, <b>24</b> )	71	(200, 130, <b>3</b> )
$F^*$	0.92	( $1.5 \cdot 10^4$ , 8100, <b>190</b> )	2.2	(6500, 1400, <b>34</b> )
$J^*$	0.76	( $1.9 \cdot 10^4$ , 3700, <b>88</b> )	0.85	( $1.7 \cdot 10^4$ , 610, <b>15</b> )

**Table 5:** Expected integrated flux  $\Phi(E > E_0)$  for our neutralino benchmark models (in units of  $10^{-15}$  ph  $\text{cm}^{-2} \text{s}^{-1}$ ), where we used the experimental parameters listed in Table 2. In parentheses, we state the increase in the signal that would be needed for a  $5\sigma$  detection as (B1,B2,**B3**). Here, B1 is the often cited increase that is needed when simply comparing the sensitivity and annihilation fluxes above the telescope energy threshold  $E_0$ .  $B2$  is more realistic in that it gives the corresponding quantity *above a certain energy  $E^*$ , depending on the benchmark, where the integrated flux to sensitivity ratio is greatest* and **B3** is the same as  $B2$ , yet for the most favourable halo profile consistent with current observations (still not taking into account the effect of substructures, however). See text for further details.

(referred to as B1 in the table). While it is customary to quote sensitivities and actual fluxes above  $E_0$  in this kind of analysis, we recall that DM annihilation spectra are rather hard, in particular when taking into account possible spectral features at photon energies close to the spectral cutoff at the mass of the DM particle. On the other hand, the sensitivity of IACTs is considerably better at energies somewhat larger than the telescope energy threshold. We therefore take the projected sensitivities for the integrated flux above some energy  $E^* > E_0$ , using the sensitivity curves as provided by Bernlöher et al. [57] for CTA and Carmona et al. [56] for MAGIC II and, by comparing those to the annihilation spectra, compute the *minimal* increase in the normalisation that is required to see at least part of the DM annihilation spectrum above  $E^*$ . This is referred to as the quantity  $B2$  in Table 5; finally, we also state as **B3** the corresponding value for the most favourable *smooth* halo profile that is consistent with the observational data (i.e. here we take the upper limit on  $\tilde{J}$  as discussed in Section 4.1).

So far, we have only discussed smooth DM distributions. On the other hand, it is well known from both theory [73] and numerical  $N$ -body simulations [74] that cold DM is expected to cluster and thereby to form substructures with masses all the way down to the small-scale cutoff in the spectrum of matter density fluctuations, which can be determined to a great accuracy from the underlying DM model [75]; if surviving until today, such inhomogeneities in the DM distribution would greatly enhance the DM annihilation rate [76]. For the case of typical dSphs, this could result in an additional boost of the signal by a factor of 10-100 [21]. Another considerable boost in

the annihilation flux could also result from the existence of a hypothetical black hole at the center of the dwarfs [19]. In the most optimistic astrophysical configuration, the required increase stated as **B3** in Table 5, would thus further be *reduced* by up to two orders of magnitude.

Let us now discuss some details of the results:

- *Sources.* For Draco, the model-dependent fluxes for the Burkert and NFW profiles are very similar, and therefore we presented only the latter in Table 5. For the astrophysical benchmark profiles introduced in Section 4.1, detectional prospects for Draco and Willman 1 only differ by a factor of around 2, and are obviously not very encouraging. When considering the most optimistic astrophysical configurations, adopting the highest observationally allowed value for  $\tilde{J}$ , things change considerably and Willman 1 becomes an interesting and indeed very promising target for DM searches. Allowing for an additional, in fact well-motivated, boost due to the presence of DM substructures in the dwarfs, this may give at least CTA the chance to see also Draco in some cases.
- *Telescopes.* Depending on the DM model, the ability of CTA to detect gamma rays from DM annihilation is a factor of 6 – 8 better than for MAGIC II. Focusing on Willman 1, and assuming very favourable astrophysical conditions, CTA would in principle be able to see *all* the benchmark models considered here, while MAGIC II should be able to see at least some of them. We recall that the flux enhancements needed for a  $5\sigma$  detection, as states in Table 5, are calculated with respect to an observation time of  $t_{obs} = 50$  hrs and scale like  $t_{obs}^{-1/2}$ . For prolonged observation times, one could thus win a factor of a few for both telescopes. Furthermore, as the CTA parameters are still quite preliminary, an additional factor of 2 in the sensitivity of the operating instrument seems quite feasible.
- *Benchmark models.* The best prospects for detection are found for the neutralino in the funnel region (model  $K'$ ), the reason simply being a rather large annihilation rate. The second-best prospects are found for model  $J^*$  in the coannihilation region. Recalling from Table 4 that  $J^*$  is actually the model with the *smallest* annihilation rate, this may come as some surprise and nicely illustrates the importance of including IB contributions when estimating the flux from DM annihilation. The model  $F^*$  is yet another example with rather pronounced IB contributions; a mass of almost 2 TeV, however, efficiently suppresses the annihilation flux (in this case, the required boost actually depends significantly on the details of the — so far not sufficiently well known — integrated sensitivity of CTA for TeV photons and could thus eventually be significantly improved).

When compared to previous work, we thus arrive at considerably more optimistic conclusions than what has been reached by Sanchez–Conde et al. [20] for the analysis of present-day gamma ray telescopes – not the least due to our fully taking into account all the contributions to the expected annihilation spectrum. On the other hand, we find the conclusions of Strigari et al. [52] overly optimistic, a fact that we trace back to the very large particle flux factor of  $\Phi^{PP} = 5 \times 10^{-29} \text{cm}^3 \text{s}^{-1} \text{GeV}^{-2}$  that the authors assumed as a fiducial value (this should be compared to Table 4 and the corresponding values for our benchmark models, which represent typical neutralino DM candidates). While it may indeed be possible to find DM models with higher gamma

ray yields than considered here, we recall that there exist rather tight general bounds on the allowed annihilation cross section and the number of high-energy photons that are produced [77]. Finally, we would like to remark that it is certainly promising to combine the DM searches in gamma rays, as described here, with observations of the same dSphs at other wavelengths (see also [19, 78]).

## 6. Conclusions

In this article, we have computed the prospects of detecting gamma rays from annihilating DM in two nearby dwarf galaxies, Draco and Willman 1, for the upcoming ground-based Imaging Atmospheric Cherenkov Telescopes MAGIC II and the CTA telescope array (the latter still being in the early design phase). We have focused our analysis on a set of five benchmark models, representatives for the parameter space of neutralino DM in the mSUGRA framework, and paid special attention to describing those telescope features that are most relevant in this context. For the first time in this kind of analysis, we have fully taken into account the contributions from radiative corrections that were recently reported by Bringmann et al. [27]. As it turned out, in fact, taking realistic DM spectra has an important impact on the analysis and, although common practice, *it can be a rather bad approximation to simply assume a featureless DM spectrum like from  $b\bar{b}$  fragmentation and/or to only focus on the total flux above a given energy threshold  $E_0$*  in these kind of studies. The basic underlying reason for this is that *realistic DM annihilation spectra show a harder energy dependence than the sensitivity of IACTs*. Once detected, clear spectral features would, of course, have the additional advantage of providing a rather fool-proof way of discriminating DM spectra against astrophysical background sources – which is even more important in view of the still rather large astrophysical uncertainties involved.

Although these effects do provide a considerable enhancement of the detectional prospects, the expected flux from dSphs remains at a level that, for conservative scenarios, will be challenging to detect with the next generation of IACTs. This, rather than the angular resolution of these instruments, is the reason why the potential of IACTs to discriminate between different DM profiles in dSphs is limited even in the case of the detection of an annihilation signal; the eventual disentanglement between cored and cuspy profiles is probably more promising to perform at other wavelengths.

On the other hand, if one adopts the most optimistic astrophysical configurations that are compatible with current observational data of Willman 1, i.e. a favourable DM profile and an  $O(10 - 100)$  flux enhancement due to the existence of substructures, *all* of our benchmark models approach the reach of at least the CTA which, for the models studied here, is a factor of 6 – 8 more sensitive to the annihilation signal than MAGIC II (this is, of course, independent of the source). The most promising case of our analysis turns out to be a neutralino in the funnel region, characterised by no sizeable IB contributions to its spectrum but a rather large annihilation rate; the second best case is a neutralino from the coannihilation region, making up for its small annihilation rate with enormously large radiative corrections.

Having demonstrated that the prospects of indirect DM detection through gamma rays do depend on the details of the annihilation spectrum, and thus the underlying particle nature, it would be interesting to perform similar analyses also for other targets of potential DM annihilation. Another further direction of extending the present analysis would be to perform a full scan over the param-

eter space of viable models. Finally, we have stressed that the very concept of sensitivity of an IACT depends on the spectrum that is observed; in the context of DM searches, this is particularly important as DM annihilation spectra can significantly deviate from the usually assumed Crab-like spectrum. While we have provided a first estimate of how to proceed in such a case, it would be warranting to perform a dedicated analysis, using the full power of state-of-the-art MC tools, in order to accurately determine the importance of this effect.

Finally, we would like to mention that even in the case of negative detection, IACTs could in principle put interesting upper limits on the flux which in turn would translate into constraints on the combined space of astrophysical and particle physics parameters. Though much smaller than for other sources like, e.g., the galactic center, the main uncertainty in this case lies in the overall scale of the flux as determined by the details of the DM distribution. This, unfortunately, will therefore greatly obstacle any stringent constraint from null searches on the particle physics nature of DM for quite some time ahead.

To conclude, nearby dwarf galaxies – and in particular Willman 1 – are very interesting and promising targets for DM searches with the next generation of IACTs. An excellent performance of these experiments, in particular in terms of the sensitivity at energies slightly below the DM particle mass, will be paramount in such searches. In fact, given the low level of fluxes involved, a factor of 2 in sensitivity might decide whether a signal will be seen or not. Complementary to such demanding requirements on the experiments, the above discussion should also have made clear that it will be very important to collect more astrophysical data and to improve the theoretical understanding of how DM is distributed in order to reduce the still unpleasantly large astrophysical uncertainties involved.

## Acknowledgments

We would like to thank the MAGIC collaboration and in particular G. Bertone, E. Carmona, M. Mariotti, M. Persic, L. Pieri for useful suggestions and A. Biland, D. Mazin and the anonymous referee for helpful discussions and comments on the manuscript.

*Note added:* After the completion of this work, Segue 1 has been presented as yet another ultra-faint Milky Way dwarf satellite galaxy, with an expected DM induced gamma-ray flux almost twice that of Willman 1 [14]. Our conclusions can be easily applied to this interesting newly discovered target by simply scaling the boost factors reported in Table 5 accordingly. We also mention that the MAGIC collaboration recently reported an upper limit on the observation of Willman 1 of the order of  $10^{-12}$  ph cm<sup>-2</sup>s<sup>-1</sup> above 100 GeV using the analysis method described in [79].

## References

- [1] **WMAP** Collaboration, E. Komatsu *et al.*, *Five-Year Wilkinson Microwave Anisotropy Probe WMAP. Observations: Cosmological Interpretation*, [arXiv:0803.0547](#).
- [2] G. Jungman, M. Kamionkowski, and K. Griest, *Supersymmetric dark matter*, *Phys. Rept.* **267** (1996) 195–373, [[hep-ph/9506380](#)].
- [3] L. Bergström, *Non-baryonic dark matter: Observational evidence and detection methods*, *Rept. Prog. Phys.* **63** (2000) 793, [[hep-ph/0002126](#)].

- [4] G. Bertone, D. Hooper, and J. Silk, *Particle dark matter: Evidence, candidates and constraints*, *Phys. Rept.* **405** (2005) 279–390, [hep-ph/0404175].
- [5] M. Taoso, G. Bertone, and A. Masiero, *Dark Matter Candidates: A Ten-Point Test*, *JCAP* **0803** (2008) 022, [arXiv:0711.4996].
- [6] M. Battaglia, I. Hinchliffe, and D. Tovey, *Cold dark matter and the LHC*, *J. Phys.* **G30** (2004) R217–R244, [hep-ph/0406147].
- [7] E. A. Baltz, M. Battaglia, M. E. Peskin, and T. Wizansky, *Determination of dark matter properties at high-energy colliders*, *Phys. Rev.* **D74** (2006) 103521, [hep-ph/0602187].
- [8] **XENON** Collaboration, J. Angle *et al.*, *First Results from the XENON10 Dark Matter Experiment at the Gran Sasso National Laboratory*, *Phys. Rev. Lett.* **100** (2008) 021303, [arXiv:0706.0039].
- [9] **CDMS** Collaboration, Z. Ahmed *et al.*, *A Search for WIMPs with the First Five-Tower Data from CDMS*, arXiv:0802.3530.
- [10] G. Gilmore *et al.*, *The Observed properties of Dark Matter on small spatial scales*, astro-ph/0703308.
- [11] M. Mateo, *Dwarf Galaxies of the Local Group*, *Ann. Rev. Astron. Astrophys.* **36** (1998) 435–506, [astro-ph/9810070].
- [12] G. S. Da Costa in *Proc. of The Third Stromlo Symposium: The Galactic Halo*, p. 165, 1999.
- [13] J. D. Simon and M. Geha, *The Kinematics of the Ultra-Faint Milky Way Satellites: Solving the Missing Satellite Problem*, *Astrophys. J.* **670** (2007) 313–331, [arXiv:0706.0516].
- [14] M. Geha *et al.*, *The Least Luminous Galaxy: Spectroscopy of the Milky Way Satellite Segue 1*, arXiv:0809.2781.
- [15] R. R. Munoz *et al.*, *Exploring Halo Substructure with Giant Stars VIII: The Velocity Dispersion Profiles of the Ursa Minor and Draco Dwarf Spheroidals At Large Angular Separations*, *Astrophys. J.* **631** (2005) L137–L142, [astro-ph/0504035].
- [16] A. W. McConnachie, J. Penarrubia, and J. F. Navarro, *Multiple components and the interpretation of velocity dispersion profiles in dwarf spheroidals*, astro-ph/0608687.
- [17] L. Bergström and D. Hooper, *Dark matter and gamma-rays from Draco: MAGIC, GLAST and CACTUS*, *Phys. Rev.* **D73** (2006) 063510, [hep-ph/0512317].
- [18] L. E. Strigari *et al.*, *Redefining the Missing Satellites Problem*, arXiv:0704.1817.
- [19] S. Colafrancesco, S. Profumo, and P. Ullio, *Detecting dark matter WIMPs in the Draco dwarf: a multi-wavelength perspective*, *Phys. Rev.* **D75** (2007) 023513, [astro-ph/0607073].
- [20] M. A. Sanchez-Conde *et al.*, *Dark matter annihilation in Draco: New considerations of the expected gamma flux*, *Phys. Rev.* **D76** (2007) 123509, [astro-ph/0701426].
- [21] L. E. Strigari *et al.*, *Precise constraints on the dark matter content of Milky Way dwarf galaxies for gamma-ray experiments*, *Phys. Rev.* **D75** (2007) 083526, [astro-ph/0611925].
- [22] A. A. Klypin, A. V. Kravtsov, O. Valenzuela, and F. Prada, *Where are the missing galactic satellites?*, *Astrophys. J.* **522** (1999) 82–92, [astro-ph/9901240].
- [23] B. Moore *et al.*, *Dark matter substructure within galactic halos*, *Astrophys. J.* **524** (1999) L19–L22.
- [24] J. A. R. Cembranos, J. L. Feng, A. Rajaraman, and F. Takayama, *SuperWIMP solutions to small scale structure problems*, *Phys. Rev. Lett.* **95** (2005) 181301, [hep-ph/0507150].

- [25] M. Kaplinghat, *Dark matter from early decays*, *Phys. Rev.* **D72** (2005) 063510, [astro-ph/0507300].
- [26] F. Borzumati, T. Bringmann, and P. Ullio, *Dark matter from late decays and the small-scale structure problems*, *Phys. Rev.* **D77** (2008) 063514, [hep-ph/0701007].
- [27] T. Bringmann, L. Bergström, and J. Edsjö, *New Gamma-Ray Contributions to Supersymmetric Dark Matter Annihilation*, *JHEP* **01** (2008) 049, [arXiv:0710.3169].
- [28] A. G. Wilson in *Publications of the Astronomical Society of the Pacific*, vol. 67, p. 27. Chicago Journals, 1954.
- [29] M. Aaronson *Astrophys. J.* **266** (1983) L11.
- [30] M. Shetrone, P. Cote, and W. L. W. Sargent, *Abundance Patterns in the Draco, Sextans and Ursa Minor Dwarf Spheroidal Galaxies*, *Astrophys. J.* **548** (2001) 592–608, [astro-ph/0009505].
- [31] A. Aparicio, R. Carrera, and D. Martinez-Delgado, *The Star Formation History and the Morphological Evolution of the Draco Dwarf Spheroidal Galaxy*, *Astronom. J.* **123** (2002) 2511, [astro-ph/0108159].
- [32] S. Piatek, C. Pryor, T. E. Armandroff, and E. W. Olszewski, *Structure of the Draco Dwarf Spheroidal Galaxy*, astro-ph/0201297.
- [33] M. Segall, R. Ibata, M. Irwin, N. Martin, and S. Chapman, *Draco, a flawless dwarf galaxy*, *Mon. Not. Roy. Astron. Soc.* **375** (2007) 831–842, [astro-ph/0612263].
- [34] M. G. Walker *et al.*, *Velocity Dispersion Profiles of Seven Dwarf Spheroidal Galaxies*, arXiv:0708.0010.
- [35] J. F. Navarro, C. S. Frenk, and S. D. M. White, *A Universal Density Profile from Hierarchical Clustering*, *Astrophys. J.* **490** (1997) 493–508, [astro-ph/9611107].
- [36] C. Tyler, *Particle dark matter constraints from the Draco dwarf galaxy*, *Phys. Rev.* **D66** (2002) 023509, [astro-ph/0203242].
- [37] S. Kazantzidis *et al.*, *Density Profiles of Cold Dark Matter Substructure: Implications for the Missing Satellites Problem*, *Astrophys. J.* **608** (2004) 663–679, [astro-ph/0312194].
- [38] E. L. Lokas, G. A. Mamon, and F. Prada, *Dark matter distribution in the Draco dwarf from velocity moments*, *Mon. Not. Roy. Astron. Soc.* **363** (2005) 918, [astro-ph/0411694].
- [39] S. Mashchenko, A. Sills, and H. M. P. Couchman, *Constraining global properties of the Draco dwarf spheroidal galaxy*, *Astrophys. J.* **640** (2006) 252–269, [astro-ph/0511567].
- [40] V. Springel *et al.*, *The Aquarius Project: the subhalos of galactic halos*, arXiv:0809.0898.
- [41] A. Burkert, *The Structure of dark matter halos in dwarf galaxies*, *IAU Symp.* **171** (1996) 175, [astro-ph/9504041].
- [42] P. Salucci and A. Burkert, *Dark Matter Scaling Relations*, *Astrophys. J.* **537** (2000) 9, [astro-ph/0004397].
- [43] M. Chertok *et al.*, *Search for dark matter annihilations in Draco with CACTUS*, *AIP Conf. Proc.* **842** (2006) 995–997.
- [44] STACEE Collaboration, D. D. Driscoll *et al.*, *Search for Dark Matter Annihilation in Draco with STACEE*, arXiv:0710.3545.

- [45] M. Wood *et al.*, *A Search for Dark Matter Annihilation with the Whipple 10m Telescope*, arXiv:0801.1708.
- [46] **MAGIC** Collaboration, J. Albert *et al.*, *Upper limit for gamma-ray emission above 140 GeV from the dwarf spheroidal galaxy Draco*, *Astrophys. J.* **679** (2008) 428–431, [arXiv:0711.2574].
- [47] B. Willman *et al.*, *A New Milky Way Dwarf Galaxy in Ursa Major*, *Astrophys. J.* **626** (2005) L85–L88, [astro-ph/0503552].
- [48] B. Willman *et al.*, *Willman 1 - A Galactic Satellite at 40 kpc With Multiple Stellar Tails*, astro-ph/0603486.
- [49] **SDSS** Collaboration, D. G. York *et al.*, *The Sloan Digital Sky Survey: technical summary*, *Astron. J.* **120** (2000) 1579–1587, [astro-ph/0006396].
- [50] N. F. Martin, R. A. Ibata, S. C. Chapman, M. Irwin, and G. F. Lewis, *A Keck/DEIMOS spectroscopic survey of faint Galactic satellites: searching for the least massive dwarf galaxies*, arXiv:0705.4622.
- [51] M. H. Siegel, M. D. Shetrone, and M. Irwin, *Trimming Down the Willman 1 dSph*, arXiv:0803.2489.
- [52] L. E. Strigari *et al.*, *The Most Dark Matter Dominated Galaxies: Predicted Gamma-ray Signals from the Faintest Milky Way Dwarfs*, arXiv:0709.1510.
- [53] A. M. Hillas in *Proc. of the 19th ICRC*, (La Jolla), January, 1985.
- [54] J. Kidea *et al.* *Astropart. Phys.* **28** (2007) 182.
- [55] G. Pulhofer *et al.* in *Proc. of the 28th ICRC*, (Tsukuba, Japan), 2003.
- [56] **MAGIC** Collaboration, E. Carmona *et al.*, *Monte Carlo Simulation for the MAGIC-II System*, arXiv:0709.2959.
- [57] K. Bernloehr, E. Carmona, and T. Schweizer in *Proc. of the 30th ICRC*, (Merida, Mexico), 2007.
- [58] T. Schweizer. private communication, 2007.
- [59] N. Gehrels and P. Michelson, *GLAST: The next-generation high energy gamma-ray astronomy mission*, *Astropart. Phys.* **11** (1999) 277–282.
- [60] A. Biland in *Proc. of IDM 2008*, (Stocholm, Sweden), 2008.
- [61] W. Hofmann, *Performance limits for Cherenkov instruments*, astro-ph/0603076.
- [62] T. P. Li and Y. Q. Ma, *Analysis methods for results in gamma-ray astronomy*, *Astrophys. J.* **272** (1983) 317–324.
- [63] L. Bergström, P. Ullio, and J. H. Buckley, *Observability of gamma rays from dark matter neutralino annihilations in the Milky Way halo*, *Astropart. Phys.* **9** (1998) 137–162, [astro-ph/9712318].
- [64] N. Fornengo, L. Pieri, and S. Scopel, *Neutralino annihilation into gamma-rays in the Milky Way and in external galaxies*, *Phys. Rev.* **D70** (2004) 103529, [hep-ph/0407342].
- [65] A. Birkedal, K. T. Matchev, M. Perelstein, and A. Spray, *Robust gamma ray signature of WIMP dark matter*, hep-ph/0507194.
- [66] A. R. L. Chamseddine A. H. and N. P., *Phys. Rev. Lett.* **49** (1982) 970.
- [67] P. Gondolo *et al.*, *DarkSUSY: Computing supersymmetric dark matter properties numerically*, *JCAP* **0407** (2004) 008, [astro-ph/0406204].

- [68] F. E. Paige, S. D. Protopopescu, H. Baer, and X. Tata, *ISAJET* 7.69: A Monte Carlo event generator for  $p p$ ,  $anti-p p$ , and  $e+ e-$  reactions, [hep-ph/0312045](#).
- [69] M. Battaglia *et al.*, Updated post-WMAP benchmarks for supersymmetry, *Eur. Phys. J.* **C33** (2004) 273–296, [[hep-ph/0306219](#)].
- [70] L. Bergström, *Radiative processes in dark matter photino annihilation*, *Phys. Lett.* **B225** (1989) 372.
- [71] L. Bergström, T. Bringmann, M. Eriksson, and M. Gustafsson, *Gamma rays from heavy neutralino dark matter*, *Phys. Rev. Lett.* **95** (2005) 241301, [[hep-ph/0507229](#)].
- [72] P. Gondolo, J. Edsjö, L. Bergström, P. Ullio, M. Schelke, E. Baltz, T. Bringmann, and G. Duda, *Darksusy 5.0.1*, 2005.
- [73] A. M. Green, S. Hofmann, and D. J. Schwarz, *The first WIMPy halos*, *JCAP* **0508** (2005) 003, [[astro-ph/0503387](#)].
- [74] J. Diemand, B. Moore, and J. Stadel, *Earth-mass dark-matter haloes as the first structures in the early universe*, *Nature*. **433** (2005) 389–391, [[astro-ph/0501589](#)].
- [75] T. Bringmann and S. Hofmann, *Thermal decoupling of WIMPs from first principles*, *JCAP* **0407** (2007) 016, [[hep-ph/0612238](#)].
- [76] L. Bergström, J. Edsjö, P. Gondolo, and P. Ullio, *Clumpy neutralino dark matter*, *Phys. Rev.* **D59** (1999) 043506, [[astro-ph/9806072](#)].
- [77] G. D. Mack, T. D. Jacques, J. F. Beacom, N. F. Bell, and H. Yuksel, *Conservative Constraints on Dark Matter Annihilation into Gamma Rays*, *Phys. Rev.* **D78** (2008) 063542, [[arXiv:0803.0157](#)].
- [78] T. E. Jeltema and S. Profumo, *Searching for Dark Matter with X-ray Observations of Local Dwarf Galaxies*, [arXiv:0805.1054](#).
- [79] **MAGIC** Collaboration, E. Aliu *et al.*, *MAGIC upper limits on the VHE gamma-ray emission from the satellite galaxy Willman 1*, [arXiv:0810.3561](#).